Twelfth Australasian Fluid Mechanics Conference
The University of Sydney, Australia 1995

NUMERICAL SIMULATION OF LOW-MACH-NUMBER COMPRESSIBLE FLOWS

Chin-Hsien Li
CSIRO Division of Mathematics & Statistics
Sydney, NSW
Australia

ABSTRACT

Based upon the operator splitting method designed by the author to solve Navier-Stokes equations with variable density and viscosity, a segregated time marching solution scheme is proposed for solving the low-Mach-number flow model with the acoustic waves being filtered out. This solution scheme does not rely on the correction for global mass conservation to mantain solution accuracy. With this advantage, the scheme can be directly applied to general low-Mach-number flow problems with confidence.

The scheme is validated by comparing the results for a number of test cases with known exact solutions and published numerical solutions by other authors.

GOVERNING EQUATIONS

By separating pressure p into a thermodynamic part p_T which is spatially uniform and a hydrodynamic part p_d, the non-dimensionalized governing equations for low-Mach-number flows can be written in the following form (see [2],[3]):

Navier-Stokes equation:

$$\rho\frac{Du_i}{Dt} - \sum_{j=1}^{N}\frac{\partial}{\partial x_j}[\mu(\frac{\partial u_i}{\partial x_j}+\frac{\partial u_j}{\partial x_i})] + \frac{\partial p_d}{\partial x_i} = -\frac{1}{\beta_r \delta T}(\rho - \sqrt{Ra/Pr})\, n_i,\ i=1,\ldots,N \quad (1)$$

$$\nabla\bullet\mathbf{u} = W(Z,\mathbf{u}) \quad (2)$$

Heat equation:

$$\rho\, Pr\frac{DT}{Dt} - \sum_{j=1}^{N}\frac{\partial}{\partial x_j}[k\frac{\partial T}{\partial x_j}] = \frac{dp_T}{dt} + Q \quad (3)$$

Equation of State:

$$\rho = \frac{R_o p_T}{1+\beta_r\delta T\cdot T} \quad (4)$$

O.D.E. for p_T:

$$meas(\Omega)\frac{dp_T}{dt} + (\int_\Omega \nabla\bullet\mathbf{u}\, d\mathbf{x})\, p_T = \frac{\gamma-1}{\gamma}\, Pr\int_\Omega \rho\frac{DT}{Dt}\, d\mathbf{x} \quad (5)$$

where

$$Z = \ln\rho \ \ and \ \ W(Z,\mathbf{u}) = -[\frac{\partial Z}{\partial t} + (\mathbf{u}\bullet\nabla)Z]$$

The notations used here are: Pr—Prandtl number, Ra—Rayleigh number, $\beta_r = 1/T_r$ with T_r—representative temperature, δT—temperature variation scale, $n_i = \delta_{i3}$ with δ_{ij}—Kronecker delta function, $R_o = \frac{\sqrt{Ra/Pr}}{R_T}$ with $R_T = \frac{\sqrt{RaPr}}{\beta_r\delta T}\frac{\gamma-1}{\gamma}$, $\gamma = C_p/C_v$ (=1.4 for air). In general, the conductivity k and viscosity μ are functions of temperature T. In this paper we assume they are of the Sutherland law forms for air (see [1],[2]).

Note that since the dynamic pressure p_d in the momentum equation is now not related to density variation, this model does not contain acoustic waves.

SOLUTION BY SEGREGATED TIME STEPPING

Let $\{T^n, \mu^n, k^n, p_T^n, \rho^n, Z^n, \mathbf{u}^n, p_d^n\}$ be the known solution values at the time level $t^n = n\Delta t$, the segregated time stepping scheme we propose for solving the nondimensionalized models (1)-(5) proceeds as follows:

1) Solve for T^{n+1} the heat equation

$$\rho^n Pr\frac{\partial T}{\partial t} + \rho^n Pr(\mathbf{u}^*\bullet\nabla)T - \sum_{j=1}^{N}\frac{\partial}{\partial x_j}[k^n\frac{\partial T}{\partial x_j}] = Q + \frac{p_T^n - p_T^{n-1}}{\Delta t} \quad (6)$$

by either fully implicit (backward Euler) scheme or Crank-Nicolson scheme. $\mathbf{u}^*$ here, may be taken as $\mathbf{u}^n$, or the extrapolation: $2\mathbf{u}^n - \mathbf{u}^{n-1}$ for Euler scheme or $(3\mathbf{u}^n - \mathbf{u}^{n-1})/2$ for Crank-Nicolson scheme.

2) Calculate $\mu^{n+1} = \mu(T^{n+1})$ and $k^{n+1} = k(T^{n+1})$.

3) Solve for p_T^{n+1} the O.D.E. (5) by either fully implicit (backward Euler) scheme or Crank-Nicolson scheme. Let

$$V = meas(\Omega),\quad F^* = \int_\Omega \nabla\bullet\mathbf{u}^*\, d\mathbf{x},$$

$$S^* = \frac{\gamma-1}{\gamma}\, Pr\int_\Omega \rho^n\{\frac{T^{n+1}-T^n}{\Delta t} + (\mathbf{u}^*\bullet\nabla)T^*\}\, d\mathbf{x}$$

T^* here denotes T^{n+1} for Euler scheme and $(T^{n+1}+T^n)/2$ for Crank-Nicolson scheme. $\mathbf{u}^*$ is defined as above.

The **fully implicit** scheme is:

$$V\frac{p_T^{n+1}-p_T^n}{\Delta t} + F^*\, p_T^{n+1} = S^* \quad (7)$$

The **Crank-Nicolson** scheme is:

$$V\frac{p_T^{n+1}-p_T^n}{\Delta t}+\frac{F^*}{2}(p_T^{n+1}+p_T^n) = S^* \qquad (8)$$

4) Calculate $\rho^{n+1}=\rho(p_T^{n+1},T^{n+1})$, $Z^{n+1}=\ln\rho^{n+1}$.

5) Calculate $\rho^{n+\frac{1}{2}}=\frac{1}{2}(\rho^{n+1}+\rho^n)$, $Z^{n+\frac{1}{2}}=\ln\rho^{n+\frac{1}{2}}$.

6) Solve for $\{\mathbf{u}^{n+1},p_d^{n+1}\}$ the following Navier-Stokes equation with variable density and viscosity by operator splitting method (see [4],[5],[6]):

$$\rho^{n+\frac{1}{2}}\frac{\partial u_i}{\partial t}-\sum_{j=1}^{N}\frac{\partial}{\partial x_j}[\mu^{n+1}(\frac{\partial u_i}{\partial x_j}+\frac{\partial u_j}{\partial x_i})] +\rho^{n+\frac{1}{2}}(\mathbf{u}\bullet\nabla)u_i+\frac{\partial p_d}{\partial x_i} = -\frac{1}{\beta_r\delta T}(\rho^{n+\frac{1}{2}}-\sqrt{Ra/Pr})\,n_i,\ i=1,\ldots,N \qquad (9)$$

$$\nabla\bullet\mathbf{u} = -[\frac{Z^{n+1}-Z^n}{\Delta t}+(\mathbf{u}\bullet\nabla)Z^{n+\frac{1}{2}}] \qquad (10)$$

NUMERICAL RESULTS

Consider the natural convection of perfect gas in a vertical slot of width L and height H with left and right wall temperatures of T_h and T_c, respectively, where $T_h > T_c$. Let $T_r=(T_h+T_c)/2$, $\delta T=T_h-T_c$, aspect ratio $A=H/L$, $\epsilon=\frac{\delta T}{2T_r}$. Due to the limitation of space, we will only present results for four test cases. In the following, we denote the solution obtained with correction to p_T^{n+1} for mass conservation by A-sln, and solution without correction by B-sln.

In cases 1 and 2, our results are compared with the exact solution data (see [1]). In Tables 1 and 2 below, the critical point x-coordinates X_1, X_0, X_p, X_n on the midsection $y=A/2$ of the slot are defined as follows:

$X_1\cdots T=0$; $X_0\cdots$ velocity y-component $u_y=0$;
$X_p\cdots u_y=u_{y,max}$; $X_n\cdots u_y=u_{y,min}$.

Case 1. We consider a closed slot, i.e. with both ends closed, and choose $\epsilon=0.6$, $A=10$, $Ra=10^3$, $Pr=0.71$, $T_r=300^\circ K$. Both A-sln. and B-sln. are shown in Table 1 and Figures 1.1 and 1.2. A graded mesh of 720 rectangular elements with 2305 nodes is used for this problem. Without correction to p_T^{n+1}, the resulted deviation from mass conservation is less than 0.8%. Table 1 and Figures 1.1 and 1.2 show that the solution is not sensitive to this small deviation. The difference between the two solutions is less than 0.8%. Compared with the exact solution, both solutions are quite accurate with errors less than 2%, which is smaller than the difference of 3% between the exact solution and the numerical Navier-Stokes solution reported by Chenoweth & Paolucci (see [1]). This shows that our algorithm, does not rely on the correction to p_T^{n+1} for global mass conservation to maintain solution accuracy, therefore it can be applied to more general cases where such a correction is either impossible or unfeasible.

Case 2. We consider an open slot, i.e. with both ends open, and choose $\epsilon=0.6$, $A=10$, $Ra=10^3$, $Pr=0.71$, $T_r=300^\circ K$. The results are shown in Table 2 (denoted by V-sln.) and Figures 2.1 and 2.2.

Note that the profiles shown by Figures 1.1, 1.2, 2.1 and 2.2 are very close to those of exact solutions (see [1]).

	exact sln.	A-sln.	B-sln.	error in B
X_1	0.6360	0.6374	0.6374	0.2%
X_0	0.6360	0.6374	0.6374	0.2%
X_p	0.2900	0.2894	0.2894	0.2%
X_n	0.8730	0.8851	0.8851	1.4%
$u_{y,max}$	0.0992	0.0981	0.0974	1.8%
$u_{y,min}$	-0.0938	-0.0927	-0.0920	1.9%

TABLE 1.

	exact sln.	V-sln.	error in V-sln.
X_1	0.63600	0.63740	0.2%
X_0	0.63600	0.63740	0.2%
X_p	0.29000	0.28940	0.2%
X_n	0.87300	0.88510	1.4%
$u_{y,max}$	0.09846	0.09845	0.01%
$u_{y,min}$	-0.09615	-0.09618	0.03%

TABLE 2.

Case 3. We consider a closed sqare ($A=1$) with $\epsilon=0.6$, $Ra=10^6$, $Pr=0.71$, $T_r=300^\circ K$, compare our results with Chenoweth & Paolucci's (see [2]). A graded mesh of 576 rectangular elements with 1825 nodes used for this problem. Figiures 3.1 and 3.2 show that our results are very close to Chenoweth & Paolucci's.

Case 4. As in case 1, we consider a closed slot with $\epsilon=0.6$, $A=10$, $Pr=0.71$, $T_r=300^\circ K$ but with $Ra=10^5$. A graded mesh of 2160 rectangular elements with 6709 nodes is used for this problem.

As shown in Figures 4.1 and 4.2, the A-sln. and B-sln. are almost identical. In fact, without correction, the deviation from global mass balance is less than 0.35%, and the difference between the two solutions is also less than 0.35%. This shows again that our algorithm does not rely on the correction to p_T^{n+1} for global mass conservation to maintain solution accuracy.

Note that Figures 4.1 shows clearly a steady state with only one primary vortex. However, Chenoweth & Paolucci (see [2]) reported that the same problem has a steady state with two vorteces, one centered at $y=5.5$ and another at $y=2.5$. In the author's opinion, their finding may be a result of lacking good stability behavior of their numerical scheme.

REFERENCES

1 Chenowenth, D.R., Paolucci, S., 1985, "Gas flow in vertical slots with large horizontal temperature differences", *J. Fluid Mech.*, **28**, pp. 2365-2374.

2 Chenowenth, D.R., Paolucci, S., 1986, "Natural convection in an enclosed vertical air layer with large horizontal temperature differences", *J. Fluid Mech.*, **169**, pp. 173-210.

3 Horibata, Y., 1992, "Numerical simulation of a low-Mach-number flow with a large temperature variation", *Computers Fluids*, **21**, No. 2, pp. 185-200.

4 Dean, E., Glowinski, R., Li, C.H., 1988, "Application of Operator Splitting Methods to the Numerical Solution of Nonlinear Problems in Continuum Mechanics and Physics", Mathematics Applied to Science, ed. J. Goldstein, S. Rosecrans and G. Sod.

5 Li, C.H., 1991, "Numerical solution of Navier-Stokes equation by operator splitting", *Proceedings of the Six International Conference in Australia on Finite Element Methods*, 1, pp. 205-214.

6 Li, C.H., 1991, "On the numerical simulation of incompressible viscous flow by operator splitting", Technical Report DMS-C 91/12.

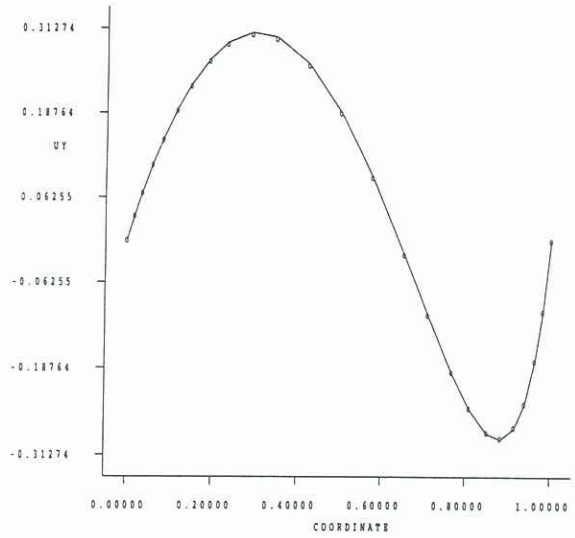

Figure 1.1 Velocity profile along $y = 5$:
solid line $\cdots$ A-sln., circules $\cdots$ B-sln.

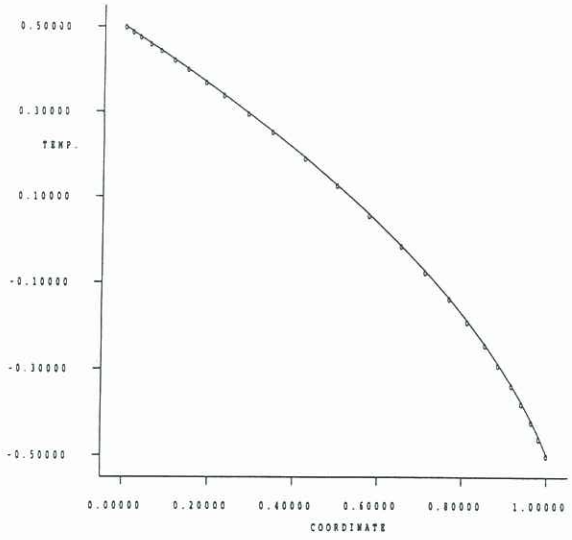

Figure 1.2 Temperature profile along $y = 5$:
solid line $\cdots$ A-sln., circules $\cdots$ B-sln.

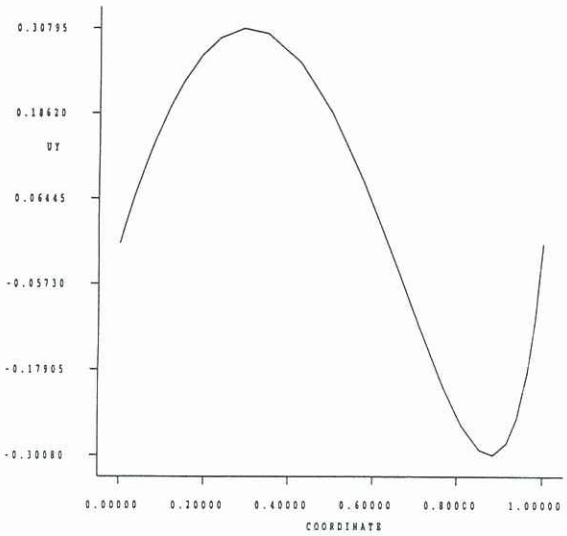

Figure 2.1 Velocity profile along $y = 5$.

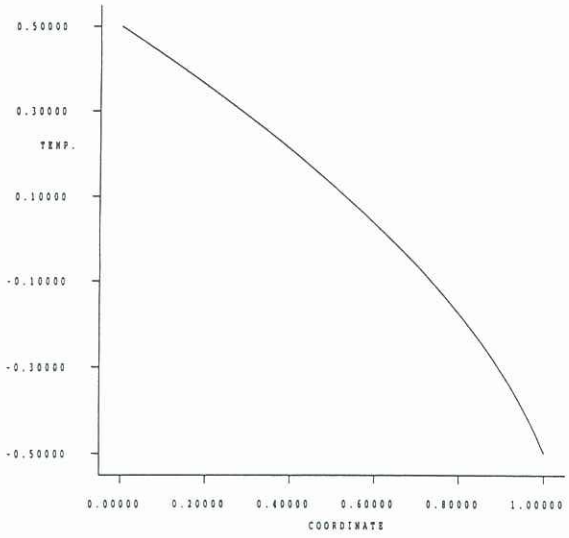

Figure 2.2 Temperature profile along $y = 5$.

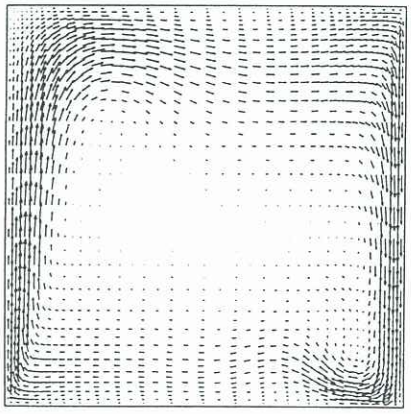

Figure 3.1(a) Velocity fields: our result

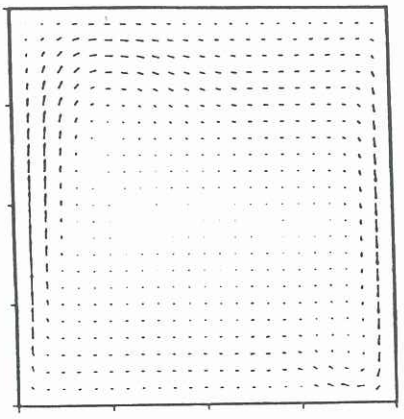

Figure 3.1(b) Velocity fields: Chenoweth & Paolucci's

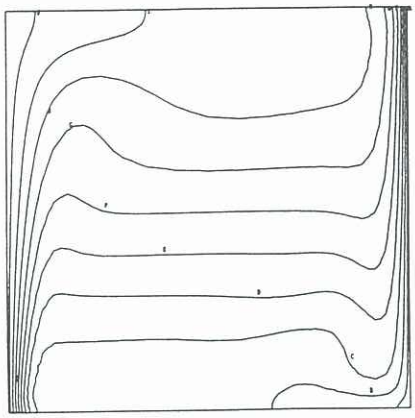

Figure 3.2(a) Isotherm fields: our result

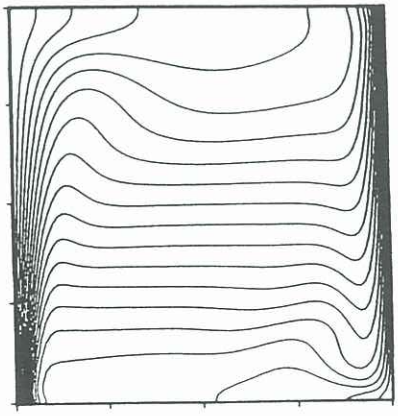

Figure 3.2(b) Isotherm fields: Chenoweth & Paolucci's

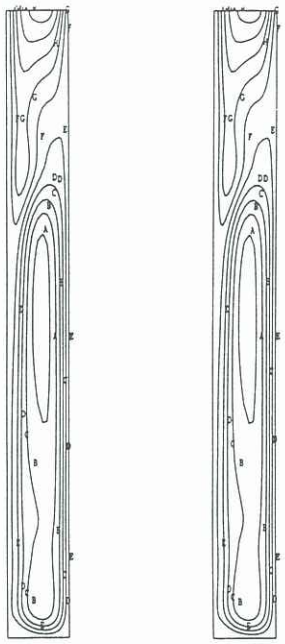

Figure 4.1 Stream lines:
left ··· A-sln., right ··· B-sln.

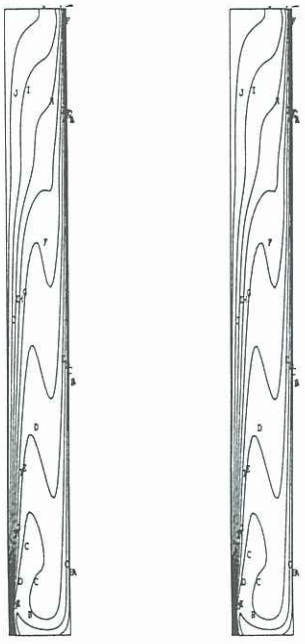

Figure 4.2 Isotherm fields:
left ··· A-sln., right ··· B-sln.